DOI: 10.1002/chem.201001888

Molecular Mechanisms of Aluminum Oxide Thin Film Growth on Polystyrene during Atomic Layer Deposition

Manjunath Puttaswamy,[a] Kenneth Brian Haugshøj,[b] Leif Højslet Christensen,[b] and Peter Kingshott*[a]

Atomic layer deposition (ALD) is a variation of the chemical vapor deposition (CVD) process, in which two gas-phase precursors are alternately exposed to the substrate. The growth occurs through self-limiting surface reactions and results in deposition of conformal ultra-thin films even on high-aspect ratio structures.[1–6] The growth of an Al_2O_3 ALD film occurs by exposure of a hydroxylated surface to two gas-phase precursors, that is, trimethylaluminum (TMA) and water vapor (H_2O), in a four-step reaction cycle as shown in Figure 1.

The four-step Al_2O_3 ALD reaction cycle is considered equivalent to one ALD reaction cycle (RC). The thickness of the ALD film is controlled by the number of RCs employed. The accurate control over the thickness of the ALD process allows deposition of nanocoatings on materials ranging from synthetic polymers to films of biomolecules.[7–9] More importantly, the application of inorganic coatings on polymers is seen, for example, as an effective barrier against H_2O and O_2 permeation, creation of scratch-resistant materials, and as an interlayer for making super-hydrophobic surfaces.[10,11]

The details of the interactions of ALD precursors, for instance, TMA and water vapor, with polymers are poorly understood. George et al.[12,13] proposed physical infiltration of TMA and H_2O precursors, resulting in the growth of Al_2O_3 within the organic polymer matrix. Recently, Lee et al.[14] proposed a possible chemical interaction during infiltration of TMA and H_2O in the amorphous regions of the polymer, resulting in chemical bonds with the polymer chains. Other important examples are the interaction of TMA with C=C bonds,[15] leading to an enhanced performance of organic light-emitting diodes (OLEDs); and metallation of porphyrins by a zinc-based ALD precursor,[16] in which the chemical interaction between the zinc precursor and porphyrin, and the infiltration of the zinc precursor into the porphyrin film has been demonstrated. In spite of these studies, no direct experimental indication of infiltration and chemical reactions of TMA and H_2O with polymer matrices exists.

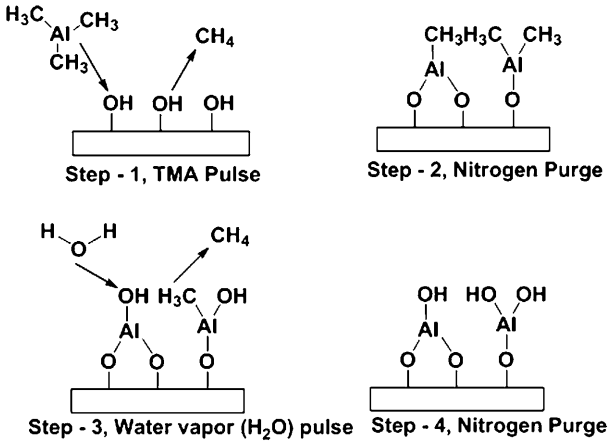

Figure 1. Four-step Al_2O_3 ALD reaction cycle (RC).

Herein, we study the Al_2O_3 ALD growth process on model polystyrene surfaces. We propose the vapor-phase infiltration of TMA and H_2O precursors in polystyrene, and also present experimental evidence of the mechanisms of the chemical reactions between the infiltrating TMA and H_2O precursors, and the polystyrene matrix (in the subsurface, i.e., a few nanometers/atomic layers beneath the surface). The polystyrene surfaces chosen include commercially available polystyrene from petri dishes, termed bulk polystyrene (BPS), and a pure polystyrene film spin-coated from

[a] M. Puttaswamy, Prof. Dr. P. Kingshott
Interdisciplinary Nanoscience Centre (iNano)
University of Aarhus, Ny Munkegade 1521-118
Aarhus C, 8000 (Denmark)
Fax: (+45) 89423690
E-mail: mputtasw@inano.au.dk

[b] K. B. Haugshøj, Dr. L. Højslet Christensen
Centre for Microtechnology and Surface Analysis
Danish Technological Institute, Gregersenvej
2630 Taastrup (Denmark)

Supporting information for this article is available on the WWW under http://dx.doi.org/10.1002/chem.201001888.

a solution in toluene, termed spin-coated polystyrene (SPS). The polystyrene surfaces were pretreated with a remote oxygen plasma source before the Al_2O_3 ALD process to generate hydroxyl groups (−OH) and other functional groups that serve as reactive sites for the TMA precursors and thus facilitate Al_2O_3 growth on the polystyrene surfaces. The Al_2O_3 ALD deposition was also performed on plain (untreated, UT) polystyrene surfaces without any plasma treatment (PT). This was done to understand the physical infiltration and chemical interactions of TMA and H_2O vapor with the polystyrene surface in the absence of reactive species. Silicon wafers (Si/SiO_2) were used as reference surfaces, which were coated at the same time as the polystyrene surfaces. The growth rate of Al_2O_3 films deposited on silicon wafer (Si/SiO_2), as measured by ellipsometry, was found to be 0.1 nm RC^{-1} (Table 1). X-ray photoelectron spectroscopy (XPS) was used to quantitatively determine the extent of Al_2O_3 deposited on each surface by monitoring the Al atomic%. Table 1 shows the Al atomic% for six different RCs.

Table 1. XPS Al atomic% obtained for six different RCs on reference silicon wafer (Si/SiO_2) and different polystyrene surfaces.

No. ALD RCs	Al atomic% on different surfaces					Thickness[a] [nm]
	Si/SiO_2	BPS-PT	SPS-PT	BPS-UT	SPS-UT	
10 RC	11.1	8.9	8.1	4.4	0	1.2
20 RC	17.2	15.6	14.2	11.3	0.6	2.1
30 RC	21.9	20.5	19.5	17.7	1.0	3.0
40 RC	24.3	23.6	23.9	23.7	18.4	4.5
120 RC	26.3	27.2	27.2	27.0	23.3	12
225 RC	34.4	34.1	34.1	33.7	30.8	20

[a] Thickness of the Al_2O_3 films on Si/SiO_2 measured by ellipsometry

The PT polystyrene surfaces (BPS-PT, SPS-PT) showed slightly lower levels of Al for the initial RCs (10, 20, and 30), in comparison with the silicon wafers (Si/SiO_2). We attribute this to a lower number of reactive sites on BPS-PT and SPS-PT surfaces (1–3 OH groups nm^{-2}),[17] than on the silicon wafer surface (5–8 OH groups nm^{-2}),[18] assuming −OH groups are the dominant reactive sites for TMA. On the other hand, among the UT polystyrene surfaces, the BPS-UT surface showed higher Al content, when compared with the SPS-UT surface. We attribute this to the low level of oxygen contamination (from oxidation or additives) present on the BPS-UT surface (see the Supporting Information for complete XPS elemental composition data, Table S1), which was sufficient to nucleate growth. For the pure SPS-UT, in which no oxygen was initially present, only a very low level of Al was detected even after 30 RCs. At higher RCs (40, 120, and 225), the Al content on BPS-PT, SPS-PT, and BPS-UT surfaces was almost the same as on silicon wafers, since the number of reactive sites presented by the Al-OH· surface could be almost the same, and at 225 RC the Al% obtained on these surfaces would be more or less equivalent to the Al% from bulk Al_2O_3. However, for the SPS-UT surface, at least 225 RCs were required to produce a level of Al% comparable to other surfaces. The slow growth of Al_2O_3 on the SPS-UT surface may be related to a slow generation of random nucleation sites through repeated cycles of TMA and water vapor. To understand the molecular interactions of TMA with the reactive sites, and the subsequent growth of Al_2O_3 as a function of increasing RC in more detail, static time-of-flight secondary ion mass spectrometry (static TOF-SIMS) analysis was performed. Static TOF-SIMS, which due to its inherent surface sensitivity (1–2 nm probe depth) and mass accuracy providing molecular specificity, is able to elucidate the reaction mechanisms that occur during the growth of Al_2O_3 on polystyrene, which to date have remained unknown for such systems. Although, secondary ions can be detected from 0–10000 amu in TOF-SIMS, we only discuss specific mass regions where unique species are detected that are indicative of reactions of TMA and H_2O with the polystyrene matrix, for increasing RCs of TMA and H_2O. The formation of a hybrid interface as a result of infiltration and reaction is subsequently tracked by using the $C_8H_7O^-$ and $C_6H_4O_2Al^-$ fragment ions, as shown in Figure 2.

The $C_8H_7O^-$ fragment ion results from the hydroxylation of the phenyl ring of polystyrene.[19,20] It was observed on BPS-PT, SPS-PT, and BPS-UT surfaces (Figure 3a). This ion forms when the polystyrene surface is oxidized during plasma treatment, and is seen on BPS-PT and SPS-PT surfaces, or when oxygen is present as a contamination (BPS-UT). However, on the SPS-UT surface, which was clean, the

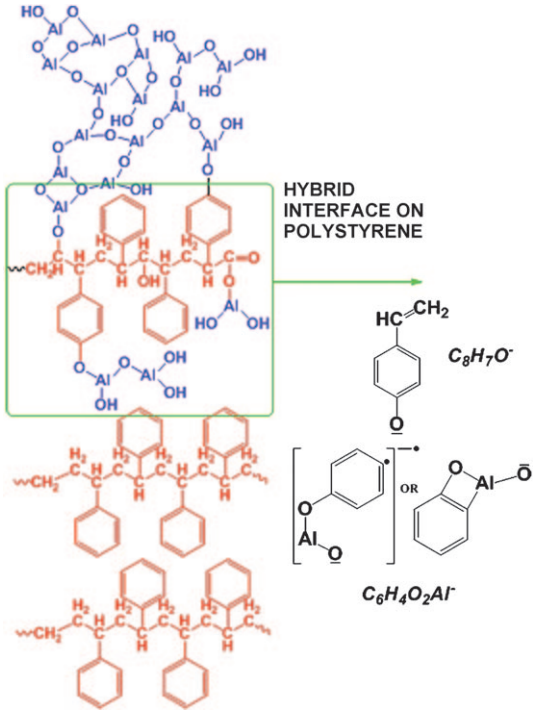

Figure 2. Proposed growth mechanism of Al_2O_3 (blue) ALD on a polystyrene (red) surface. The infiltration of TMA and H_2O precursors may result in Al_2O_3 growth in the polystyrene matrix (subsurface), and thus a hybrid interface (shown in the green box). The structure of the $C_8H_7O^-$ and $C_6H_4O_2Al^-$ ions tracking the hybrid interface on polystyrene matrix (subsurface) are also shown.

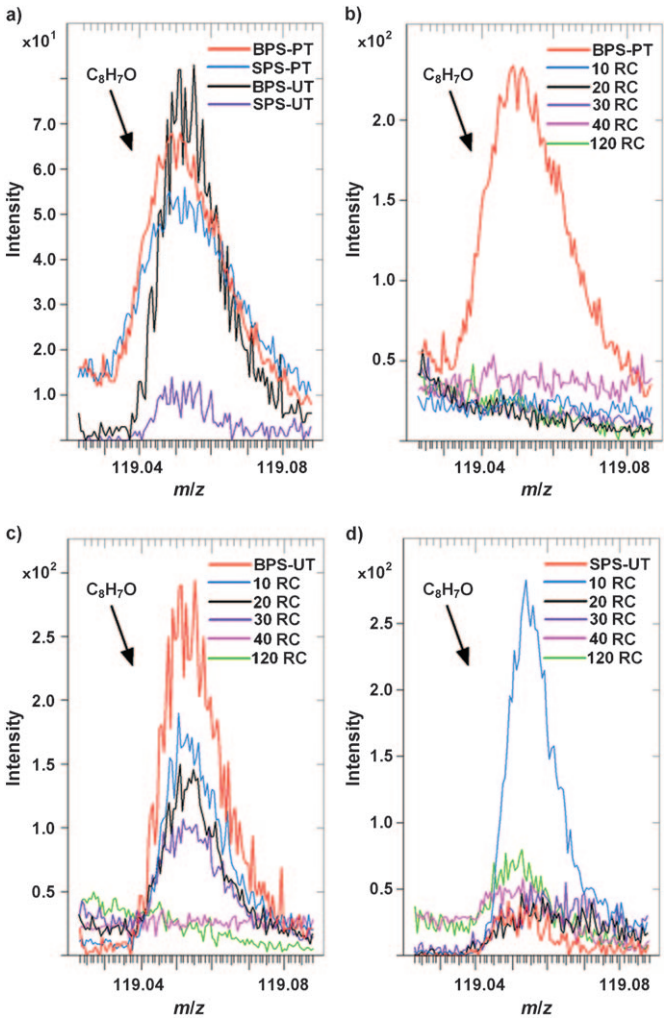

Figure 3. a) TOF-SIMS spectra showing the fragment ion $C_8H_7O^-$ recorded on the different polystyrene surfaces before Al_2O_3 ALD. Spectra for the ion $C_8H_7O^-$ detected with increasing number of RCs on b) BPS-PT c) BPS-UT, and d) SPS-UT surfaces. Note: The intensities overlaid are normalized to total ion intensity.

$C_8H_7O^-$ ion was not observed. On the BPS-PT surface, as shown in Figure 3b, the $C_8H_7O^-$ ion completely disappears after 10 RCs, indicating that this ion originates from an oxygen species that reacts completely with the TMA precursor, presumably a hydroxyl group. Similar behavior was observed on the SPS-PT surface (data not shown). For the BPS-UT surface (Figure 3c) there is a linear decrease in intensity up to 30 RCs before the signal disappears after 40 RCs. This might indicate a nonuniform (cluster) growth of Al_2O_3 on untreated polystyrene (BPS-UT) during the initial RCs, so that emission of $C_8H_7O^-$ from exposed regions of the BPS-UT surface occurs. This is also supported by the XPS results that showed lower levels of Al on the BPS-UT surface with thinner films. The TOF-SIMS data for the Al_2O_3 ALD on the SPS-UT surface (Figure 3d) where there was no starting oxygen, is quite different. The $C_8H_7O^-$ ion was detected after 10 RCs, after which time the ion intensity falls, unlike the Al_2O_3 ALD on the BPS-UT surface. We propose that during the initial RCs, TMA and H_2O cause slight oxidization of the SPS-UT surface and upon prolonged exposure TMA eventually starts to form covalent bonds with the surface. After 20 RCs the intensity of the $C_8H_7O^-$ ion almost reaches zero, yet the Al content is low. This indicates that the oxidization of the polystyrene surface is rather inhomogeneous.

Intuitively, it also indicates that there might be oxidation and simultaneous formation of covalent bonds on all polystyrene surfaces under investigation. However, the formation of new covalent bonds with the polystyrene matrix may be faster on surfaces like BPS-PT, SPS-PT, and BPS-UT, where the reactive sites already present may facilitate the retention of TMA and H_2O. The covalent bonding of infiltrating precursors (TMA and H_2O) with the polystyrene matrix (subsurface) was particularly evident during the initial (10, 20, and 30) RCs by the high-resolution core-level photoemission C 1s spectra (Figure S1a–b in the Supporting Information), where an increase in carbon–oxygen-based[21] functional groups on different polystyrene surfaces (BPS-PT/SPS-PT and BPS-UT) was observed, before the surface was saturated by signals from aluminum oxide at higher RCs (Table 1). The quantitative increase in carbon–oxygen-based functional groups, as a function of RCs on different polystyrene surfaces is tabulated in Table S2a–b in the Supporting Information. This also supports Lee et al.,[14] who proposed that infiltration of TMA and H_2O into amorphous regions may induce bond cleavage and covalent bonding, particularly when both TMA and H_2O are present. Typical characteristic substrate positive ions SiH^+ (for silicon wafer, Si/SiO_2)[22] and $C_7H_7^+$ (for polystyrene)[23] were also monitored during the initial (10, 20, and 30) RCs as shown in Figure S2a–b in the Supporting Information. The intensity of the SiH^+ ion decreased linearly, before it almost vanished at 30 RCs, indicating uniform growth. However, on BPS-UT, even after 30 RCs, where the Al% was almost comparable to the silicon wafer (Table 1), the intensity of the $C_7H_7^+$ ion was substantially higher, thus indicating infiltration. The intensities of $C_7H_7^+$ are not reported for BPS-PT and SPS-PT because there would be some degree of aromatic degradation during plasma treatment,[24] which would influence the intensities.

We also wanted to investigate the possible depth of infiltration of TMA and H_2O into the polystyrene matrix. We propose that the fragment ion $C_6H_4O_2Al^-$ can be used to track the hybrid interface on polystyrene. On the plasma-treated polystyrene surfaces (BPS-PT and SPS-PT), as shown in Figure 4a and b, the $C_6H_4O_2Al^-$ ion intensity actually increased up to 30 RCs before decreasing for 40 and 120 RCs. The gradual increase in ion intensity at low RCs (10–30), indicates possible growth of Al_2O_3 in the polystyrene matrix. However, upon higher RCs (40 and 120), there is a gradual decrease in the ion intensity, which indicates the growth of Al_2O_3 above the polystyrene surface. We also observed a similar behavior in $C_6H_4O_2Al^-$ ion intensity for Al_2O_3 growth on the BPS-UT surface as shown in Figure 4c.

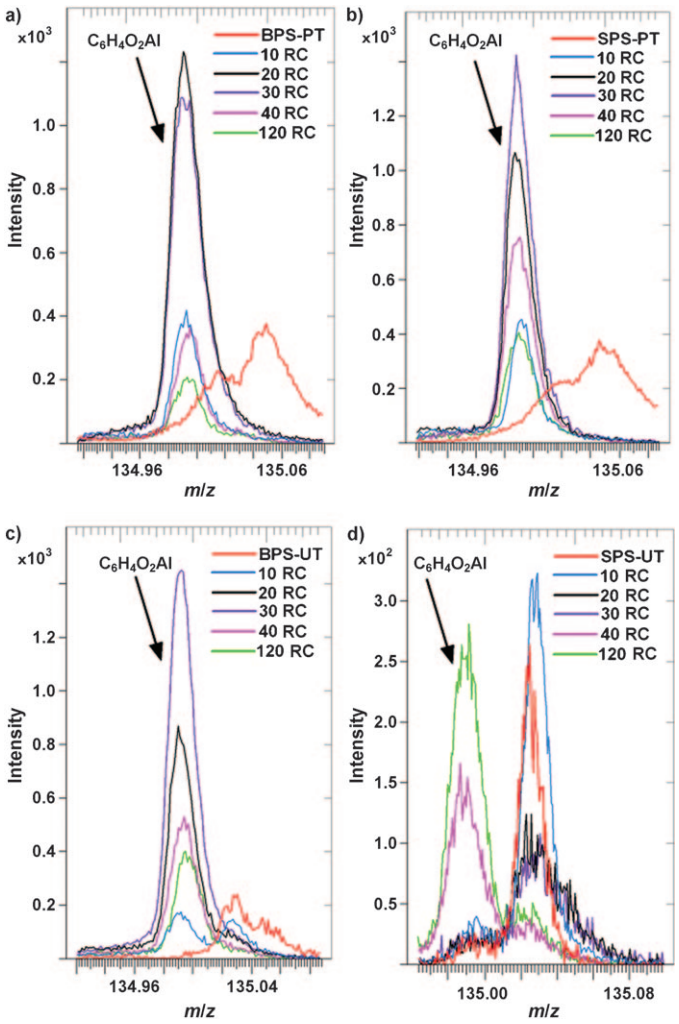

Figure 4. TOF-SIMS spectra for the $C_6H_4O_2Al^-$ fragment ion recorded on the different polystyrene surfaces with increasing number of RCs on a) BPS-PT, b) SPS-PT, c) BPS-UT, and d) SPS-UT surfaces. Note: The intensities overlaid are normalized to total ion intensity.

However on the SPS-UT surface (Figure 4d), this ion was only detected for 40 and 120 RCs. This supports our previous assumption that during the initial cycles (10–30 RCs), TMA and H_2O pulses are primarily involved in oxidizing the polystyrene surface and promoting further nucleation and growth through oxygen-based functional groups. Thus, at 40 and 120 RCs, when there was substantial growth of Al_2O_3 on SPS-UT, a gradual increase in $C_6H_4O_2Al^-$ ion intensity was observed. TOF-SIMS depth profiling (dynamic TOF-SIMS) was performed to track various ions detected from the static TOF-SIMS measurements aimed at providing supporting evidence concerning the growth of Al_2O_3 in the polystyrene matrix. The instrument cycles between etching with a Cs^+ ion source and static SIMS analysis with a Bi_3^{++} source in the etch crater, thus ion intensities versus etch time are monitored. The measurements were performed on Al_2O_3 films generated after 120 RCs, including SiO_2 as a control.

The TOF-SIMS depth profile of 120 RCs on silicon is shown in Figure 5a. As expected the AlO^- ion from the Al_2O_3 coating and the Si^- from the silicon substrate follow opposite trends with respect to intensity at the interface between Al_2O_3 and silicon. The $C_6H_4O_2Al^-$ ion was not present on the Al_2O_3 coating on silicon. However, we could track the native oxide layer (1.8 nm thick SiO_2) on the silicon wafer using the SiO_2^- ion signal, which gradually increased at the interface between Al_2O_3 and the wafer, before decaying again. On the BPS-UT surface (Figure 5b), it took longer for the AlO^- signals to reach a stable plateau

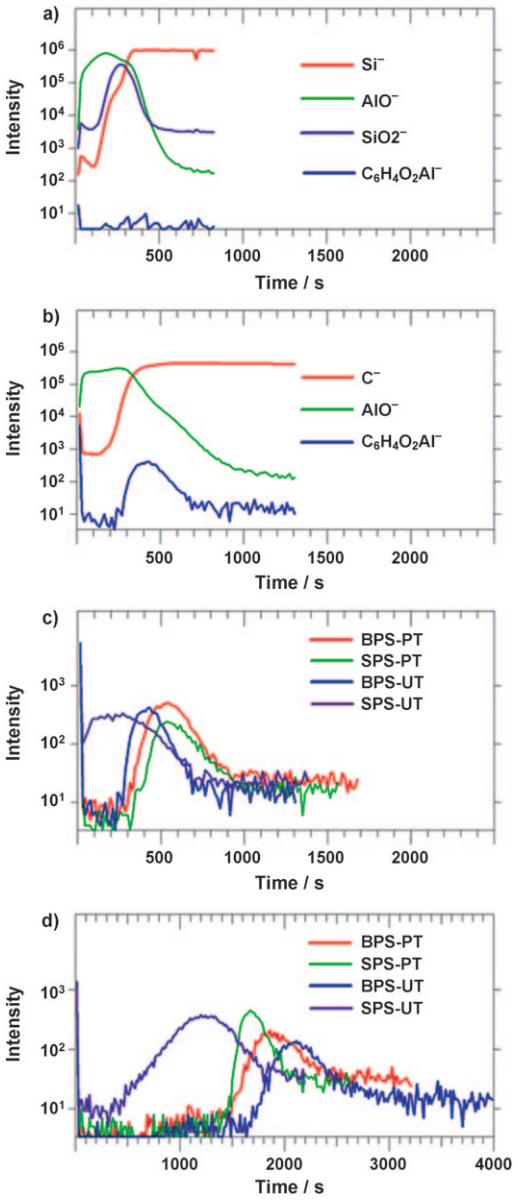

Figure 5. TOF-SIMS depth profiles for a) 120 RCs on silicon b) 120 RCs on the BPS-UT surface. c) Overlay of the $C_6H_4O_2Al^-$ signal for 120 RCs on BPS-PT, SPS-PT, BPS-UT, and SPS-UT surfaces. d) Overlay of the $C_6H_4O_2Al^-$ ion for 225 RC on BPS-PT, SPS-PT, BPS-UT, and SPS-UT surfaces.

value than on silicon, and the C^- signal from the substrate steadily increased as the Al_2O_3 was sputtered. More importantly, the intensity of the characteristic $C_6H_4O_2Al^-$ ion increases in the interface zone of the Al_2O_3 and the polystyrene surface, similar to that observed for the native oxide (SiO_2) layer on silicon, indicating the presence of Al_2O_3 in the subsurface polystyrene matrix.

The $C_6H_4O_2Al^-$ ion for 120 RCs Al_2O_3 films showed similar depth profile traces on the BPS-PT, BPS-UT, and SPS-PT substrates, as shown in Figure 5c. However, on the SPS-UT surface there was no intensity maximum in the interface zone, most likely due to nonuniform and slower rate of growth of Al_2O_3 as mentioned earlier. To track this ion on the SPS-UT surface, thicker coatings (225 RCs) were required so that it became possible to observe changes in the $C_6H_4O_2Al^-$ ion signal intensity (Figure 5d), which increased as the Al_2O_3/polystyrene interface was approached. For comparison, the $C_6H_4O_2Al^-$ ion intensity changes for the 225 RCs coating on SPS-PT, BPS-PT, and BPS-UT surfaces are also shown. Notably, the Al content, as measured by XPS for 225 RCs on all surfaces, was almost comparable. However, the depth profile for 225 RCs on the SPS-UT surface showed a slower increase in intensity of the $C_6H_4O_2Al^-$ ion, in comparison with other surfaces. We attribute this to a nonuniform, clusterlike growth of Al_2O_3 even after 225 RCs, as shown in the AFM image in Figure 6a. The corresponding image for 225 RCs on the SPS-PT surface shows a more uniform, homogeneous layer being deposited (Figure 6b) during the interaction of TMA and H_2O with polystyrene that has reactive sites.

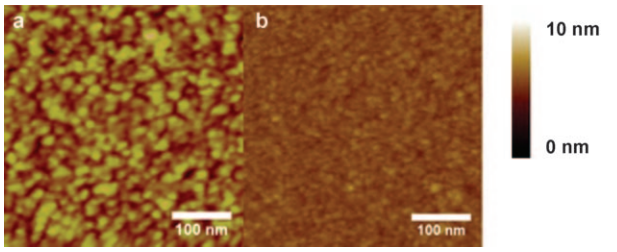

Figure 6. AFM images for 225 RCs on a) SPS-UT and b) SPS-PT surfaces.

In conclusion, we have presented novel findings demonstrating the mechanisms of growth of Al_2O_3 on polystyrene matrices resulting from infiltration and reaction of the TMA and H_2O precursors into the subsurface layers. This was qualitatively followed by tracking the depth of reaction products by using unique ions detected in TOF-SIMS spectra. Such knowledge enables the development of durable, hybrid organic/inorganic materials in which optimization of interfacial reactions is highly desirable.

Experimental Section

The experimental details are provided in the Supporting Information.

Keywords: aluminum oxides · atomic layer deposition · hybrid materials · polystyrenes · mass spectrometry

[1] T. Suntola, *Thin Solid Films* **1992**, *216*, 84.
[2] S. M. George, A. W. Ott, J. W. Klaus, *J. Phys. Chem.* **1996**, *100*, 13121.
[3] A. C. Dillon, A. W. Ott, J. D. Way, S. M. George, *Surfactant Sci. Ser.* **1995**, *322*, 230.
[4] A. W. Ott, J. W. Klaus, J. M. Johnson, S. M. George, *Thin Solid Films* **1997**, *292*, 135.
[5] M. Ritala, M. Leskela, J. P. Dekker, C. Mutsaers, P. J. Soininen, J. Skarp, *Chem. Vap. Deposition* **1999**, *5*, 7.
[6] M. L. Green, R. A. Levy, R. G. Nuzzo, E. Coleman, *Thin Solid Films* **1984**, *114*, 367.
[7] M. Knez, A. Kadri, C. Wege, U. Gosele, H. Jeske, K. Nielsch, *Nano Lett.* **2006**, *6*, 1172.
[8] L. Niinisto, J. Paivasaari, J. Niinisto, M. Putkonen, M. Nieminen, *Phys. Status Solidi A* **2004**, *201*, 1443.
[9] A. Sinha, D. W. Hess, C. L. Henderson, *J. Vac. Sci. Technol. B* **2006**, *24*, 2523.
[10] M. D. Groner, S. M. George, R. S. McLean, P. F. Carcia, *Appl. Phys. Lett.* **2006**, *88*, 051907.
[11] S. J. Yun, Y. W. Ko, J. W. Lim, *Appl. Phys. Lett.* **2004**, *85*, 4896.
[12] C. A. Wilson, R. K. Grubbs, S. M. George, *Chem. Mater.* **2005**, *17*, 5625.
[13] C. A. Wilson, J. A. McCormick, A. S. Cavanagh, D. N. Goldstein, A. W. Weimer, S. M. George, *Thin Solid Films* **2008**, *516*, 6175.
[14] S. M. Lee, E. Pippel, U. Gosele, C. Dresbach, Y. Qin, C. V. Chandran, T. Brauniger, G. Hause, M. Knez, *Science* **2009**, *324*, 488.
[15] C. Y. Chang, F. Y. Tsai, S. J. Jhuo, M. J. Chen, *Org. Electron.* **2008**, *9*, 667.
[16] L. B. Zhang, A. J. Patil, L. Li, A. Schierhorn, S. Mann, U. Gosele, M. Knez, *Angew. Chem.* **2009**, *121*, 5082; *Angew. Chem. Int. Ed.* **2009**, *48*, 4982.
[17] A. S. G. Curtis, J. V. Forrester, C. Mcinnes, F. Lawrie, *J. Cell Biol.* **1983**, *97*, 1500.
[18] E. McCafferty, J. P. Wightman, *Surf. Interface Anal.* **1998**, *26*, 549.
[19] D. M. Brewis, D. Briggs, R. H. Dahm, I. Fletcher, *Surf. Interface Anal.* **2000**, *29*, 572.
[20] X. M. Zeng, C. M. Chan, L. T. Weng, L. Li, *Polymer* **2000**, *41*, 8321.
[21] S. B. Idage, S. Badrinarayanan, *Langmuir* **1998**, *14*, 2780.
[22] A. Karen, N. Man, T. Shibamori, K. Takahashi, *Appl. Surf. Sci.* **2003**, *203*, 541.
[23] X. Vanden Eynde, P. Bertrand, J. Penelle, *Macromolecules* **2000**, *33*, 5624.
[24] J. Davies, C. S. Nunnerley, A. C. Brisley, R. F. Sunderland, J. C. Edwards, P. Kruger, R. Knes, A. J. Paul, S. Hibbert, *Colloids Surf.* **2000**, *174*, 287.

Received: July 5, 2010
Published online: November 12, 2010

